Dissipative Transport in Multigate Silicon nanowire Transistors

Nima Dehdashti, Abhinav Kranti, Isabelle Ferain, Chi-Woo Lee, Ran Yan, Pedram Razavi, Ran Yu, Jean-Pierre Colinge.
Tyndall National Institute, Cork, Ireland.
Email: nima.dehdashti@tyndall.ie

***Abstract*— Most device simulation packages performing quantum transport modeling in thin body Multigate silicon nanowire devices at nanometer scales neglect the electron-phonon interaction, assuming devices operate in the ballistic regime. Here we perform a detailed study on dissipative quantum transport in multigate silicon nanowire transistor including acoustic and optical phonons in detail using non-equilibrium Green's function formalism in uncoupled mode-space approach. We find out that g-type phonons are the most important mechanisms contributing to current reduction in multigate nanowire both in subthreshold and above threshold region for silicon nanowire with 5nm film thickness. This crucial rule of *g*-type phonons stay active even for gate lengths below 20nm, which implies that ballistic models are inadequate to capture the device characteristics of nanometre devices.**

Keywords – dissipative quantum transport, optical phonons, acoustic phonons, non-equilibrium Green's function, single band effective mass

I. INTRODUCTION

Thin-film SOI and multigate nanowire transistor structures are considered as a strong contender for the upcoming generation of ultrascaled transistors with gate length shrunk down to decananometre scales, due to outstanding control of channel electrostatics and reduction of short-channel effects [1-3]. However, the ballistic quantum transport models which have been utilised to model the devices do overestimate the drain current in both the subthreshold region and above threshold because they neglect electron-phonon interactions. Even the simple inclusion of scattering using the semiclassical Büttiker probes model is not capable of capturing the essential behaviour of electron-phonon interactions [4]. Rigorous modelling of multigate nanowire transistor structures using three-dimensional (3D) NEGF has been presented previously in [5] using the deformation potential theory and the self-consistent Born approximation. The simulation results showed the considerable reduction of 50% in drain current above threshold. However, the contribution of different electron-phonon interaction mechanisms to the current reduction has not been discussed and is still unclear. There have also been some studies on electron-phonon interaction in double-gate MOSFET and CNTFETs using NEGF formalism, where the role of acoustic phonons (AP) and optical phonons (OP) have been studied in detail [6,7]. However, due to complex band structure and the multi-subband nature of transport in a silicon nanowire, the results may differ from those obtained for CNTFET devices. Our intension in this paper is to study acoustic and optical phonons in silicon nanowires and not to compare them with other devices. In order to investigate different electron-phonon mechanisms, we have developed a three-dimensional quantum simulator based on NEGF formalism and single band effective mass Hamiltonian capable of handling different scattering processes.

We perform a detailed study of intravalley acoustic phonon scattering (AP scattering) and intervalley optical-phonon scattering (OP scattering) with different phonon energies. We show that optical phonons are more important for the typical device considered in this study. Detailed study of energy-resolved current spectrums will be also presented which reveal the current distribution inside the device and destroying of the ballistic spectrum. The observations obtained here can help the device engineers to design faster transistors with lower sub threshold swing. We will give a brief review of the simulation procedure followed by results and conclusion.

II. SIMULATION PROCEDURE

A comprehensive description on the mode-space NEGF formalism and the self-consistent Born approximation and its application to electron-phonon interaction can be found in the literature [4-7]. Here we just give a brief overview of 3D nanowire simulation in mode-space approach and its modification to consider AP and OP scattering. In mode-space framework, the three-dimensional wave function is decoupled into an energy variation in the 1D-transport direction and 2D wave function in the confinement directions. Then the 2D Schrödinger equation is solved in each cross-section to obtain the corresponding eigenvalues (modes) and eigenfunctions at each point along the transport direction. The scattering self energy parameter which includes the effect of electron-phonon wave function is taken into account by computing the electron-phonon wave function overlap (form factor). Having found the modes in each cross section and form factor, we apply the 1D NEGF quantum transport to each mode to compute the observable quantities associated with respective mode. The accuracy of uncoupled mode-space in the case of electron-phonon interaction has been justified before in the case of double-gate MOSFET and nanowire structure [5,8].

This work is supported by the Science Foundation Ireland grant 05/IN/I888: Advanced Scalable Silicon-on-Insulator Devices for Beyond-End-of-Roadmap Semiconductors. This work has also been enabled by the Programme for Research in Third-Level Institutions.

Uncoupled Mode-Space Hamiltonian

Following the method described in [3] we can build the effective mass Hamiltonian of the nanowire in uncoupled mode-space approach as follow:

$$-\frac{\hbar^2}{2}\bar{a}_{mm}(x)\frac{\partial^2}{\partial x^2}\varphi^m(x)+E^m_{sub}\cdot\varphi^m(x)=E\varphi^m(x) \tag{1}$$

where

$$\bar{a}_{mm}(x)=\oint_{y,z}\frac{1}{m^*_x}\left|\xi^m(y,z;x)\right|^2\,dydz \tag{2}$$

is the inverse of the average value of the effective mass in the cross-section. E_m and ξ are the eigenvalue and eigenfunction at position x_i; they can be calculated by solving the 2D Schrödinger equation as follow:

$$\left[-\frac{\hbar^2}{2}\frac{\partial}{\partial y}\left(\frac{1}{m^*_y}\frac{\partial}{\partial y}\right)-\frac{\hbar^2}{2}\frac{\partial}{\partial z}\left(\frac{1}{m^*_z}\frac{\partial}{\partial z}\right)+U(y,z,x_i)\right]\xi^n(y,z;x_i)=E^n_{sub}(x_i)\xi^n(y,z,x_i) \tag{3}$$

in the above equation U is the self-consistent potential at position x_i in transport direction. Having found the subbands we can set up the 1D the mode space Hamiltonian matrix and solve the NEGF equations as described in next section to compute the observable physical quantities.

Steady-State NEGF Equations

Steady-state transport equations for a single subband and a single valley in the mode-space can be written as [3-5]:

$$G^r(E)=\left[EI-H_{1D}-\Sigma_{ac}-\Sigma_{op}-\Sigma_{S,D}\right]^{-1} \tag{4}$$

$$G^{<,>}(E)=G^r\left[\Sigma^{<,>}_{ac}(E)+\Sigma^{<,>}_{op}(E)+\Sigma^{<,>}_{S,D}(E)\right]G^{r+} \tag{5}$$

where Σ_{ac} , Σ_{op} *and* $\Sigma_{S,D}$ and the self energies due to acoustic phonons, optical phonons and source/drain contacts, respectively.

Acoustic and Optical phonons self-energies

Assuming that electron-phonon interactions are local in space, we can write down the lesser and advanced scattering self-energies as follow [5-9]:

$$\Sigma^{<.>,n}_{v,ac}(E)=\left|M_q\right|^2\cdot\sum_m G^{<.>,m}_v(E)\cdot I^{n,v}_{m,v} \tag{6a}$$

$$\Sigma^{<,n}_{v,op}(E)=\left|M_q\right|^2\cdot\left(n_B+\frac{1}{2}\pm\frac{1}{2}\right)\sum_{m,v'}g^{v,v'}_j.G^{<,m}_{v'}(E\pm\hbar\omega)\cdot I^{n,v'}_{m,v} \tag{6b}$$

$$\Sigma^{>,n}_{v,op}(E)=\left|M_q\right|^2\cdot\left(n_B+\frac{1}{2}\pm\frac{1}{2}\right)\sum_{m,v'}g^{v,v'}_j.G^{>,m}_{v'}(E\mp\hbar\omega)\cdot I^{n,v'}_{m,v} \tag{6c}$$

where g_j is the phonon selection rule and M_q is the scalar electron-phonon coupling element. The expression for M_q can be found in [5]. The first and second term in (6b) and (6c) corresponds to phonon emission and absorption, respectively. Here, I is the electron-phonon overlap function across mode m,n at valley v, which is defined as [5]:

$$I^{n,v'}_{m,v}(x)=\oint\left|\xi^{n,v'}_{x,v}(y,z;x)\right|^2\cdot\left|\xi^{m,v'}_{x,v}(y,z;x)\right|^2\,dy\,dz \tag{7}$$

where ξ is the wavefunction obtained from the solution of the 2D Schrödinger equation at position $x=x_i$ as defined in (3). Finally, n_B is Bose-Einstein distribution function which is defined as [5,6]:

$$n_B(\hbar\omega)=\frac{1}{\exp(\hbar\omega/k_BT)-1} \tag{8}$$

now we can write the imaginary and real part of retarded total scattering self-energy as follow [5-7]:

$$\Im\left[\Sigma_{el-ph}(E)\right]=-\frac{i}{2}\left(\Sigma^{>}_{el-ph}(E)+\Sigma^{<}_{el-ph}(E)\right) \tag{9a}$$

$$\Re\left[\Sigma_{el-ph}(E)\right]=P\int\frac{dE'}{2\pi}\frac{\Gamma_{el-ph}(E')}{E-E'} \tag{9b}$$

it has been reported that neglecting the real part of the electron-phonon self-energy does not significantly affect the results. Hence we have ignored it in our simulations. The scattering self-energy computed from (6,9) is fed back to (4,5) to compute the new Green's function value. This procedure should be iterated until self-energy and $G^<$ reach convergence for all energy points. Once this inner convergence achieved, we check the convergence of outer loop between charge and potential. The current flowing in the nanowire from layer x_i to x_{i+1} in the transport direction can be written as follows [6-7]:

$$I^v_{x\to x+1}=\frac{q}{h}\int_{-\infty}^{+\infty}\left(H_{x,x+1}\,G^{<,v}_{x+1,x}(E)-H_{x,x+1}\,G^{<,v}_{x,x+1}(E)\right)\,\frac{dE}{2\pi} \tag{10}$$

this is a general equation which is valid for both ballistic and dissipative quantum transport equations. Energy-resolved current density can be plotted by computing (10) for each x-position independently, which has been used in this paper to study AP scattering. Also as an additional criterion, in the entire simulation we check the current continuity. The current density and criteria for current convergence can be written as [6,9]:

$$I_x=\frac{q}{h}\int_{-\infty}^{+\infty}\left(H_{x,x+1}\,G^{<}_{x+1,x}(E)\right)\,\frac{dE}{2\pi} \tag{11}$$

$$\left\|I_s-I_d\right\|\le\varepsilon \tag{12}$$

where I_s and I_d are current density at source and drain contacts and we have used an error of ε = 0.01 as convergence criterion.

III. Results and Discussion

An overview of quantum transport in 3D nanowire including elastic and inelastic electron-phonon interaction was presented in the previous section. In all the simulations we have considered self-consistency in calculation of scattering

rates and charge density. Now we discuss the effect of elastic and inelastic scattering mechanisms on the electron transport and electrical characteristics of multigate silicon nanowire. Here, we consider a trigate silicon nanowire FET transistor with <100> channel direction as presented in Fig. 1 The cross section is 5nm × 5nm. The lengths of the gate and source/drain extensions are all 10 nm. The buried oxide thickness is 5 nm and the back gate is grounded. The source and drain contacts are heavily doped N-type with N_d=10^{20} cm^{-3} while the channel region is undoped. In order to perform a detailed study of AP scattering, different gate lengths are used.

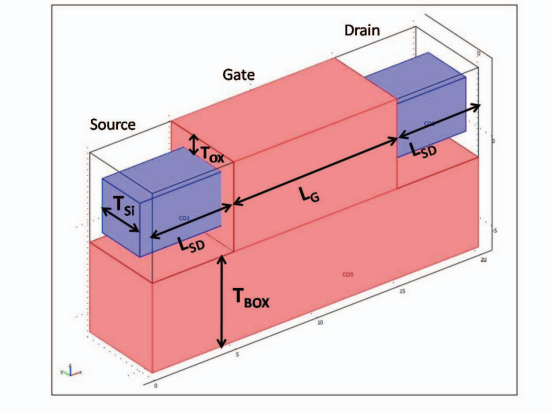

Fig. 1. Schematic presentation of the triple gate nanowire used in our simulation.

Fig. 2 presents the I_{DS}-V_{GS} curves for ballistic and dissipative transport regimes has been plotted for V_{DS}=0.4 V in both linear and log scale. It can be observed that *g*-type optical phonons are the dominant scattering mechanism in the subthreshold region and above threshold for the device under study. The *f*-type intervalley scattering involves subbands with energies higher than the lowest subband, hence they do not play any role in current reduction [10]. Now let us see how different *g*-type phonons contribute to transport and current distribution in the device. We have considered bulk phonon energies of 12, 19, 60 meV with the coupling strength M_q equal to 110, 5 and 80 MeV^2, respectively. In Fig. 3 we have plotted the contribution of individual *g*-type phonon energy on drain current reduction. We can observe that the 12 meV and 60 meV do not play any role in current reduction. This behaviour can be explained as follows. Phonons with an energy less than the thermal energy (kT) cause the back scattering of the injected carriers into source contact by phonon emission/absorption and result in drastic reduction of the drain current. On the other hand, phonons with energies larger than the thermal energy cause the injected carriers to lose energy by phonon emission and decrease the probability of the carriers to get back scattered into the source and hence less reduction in drain current is observed. With this explanation of phonon behaviour we can expect that 60 meV phonon does not contribute to current reduction as obtained by simulation results. The only two phonon modes which can contribute to drain current reduction are 12 and 19 meV phonons and hence we expect that 12 meV be the dominant phonon energy due to smaller phonon frequency. However, we should notice that the electron-phonon coupling element M_q in (6) also plays role in determining final scattering rate. With regard to higher coupling coefficient of 19 meV phonon it would be the dominant current reduction factor in silicon nanowire as obtained by the simulation results. Figs. 4 and 5 show the energy-resolved current and electron density for ballistic and different *g*-type energies. We can observe that 12 meV phonon does not have any effect on transport and output characteristics. Then we can see that 19 meV has reduced both current and electron density in the channel due to back scattering of the carriers. Finally, we can observe that high energy phonons of 60 meV have increased electron density in the channel by phonon emission without reducing the current considerably.

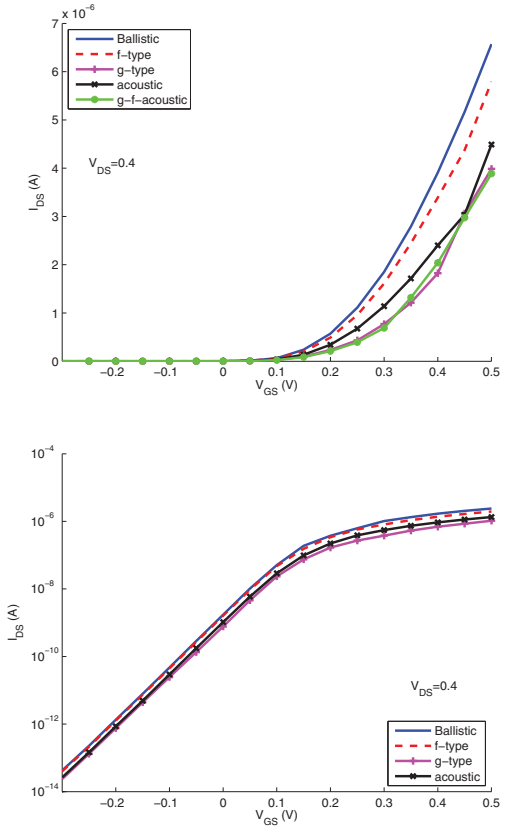

Fig. 2. I_{DS}-V_{GS} curve for L_g=30 nm in linear (top) and log scale (bottom).

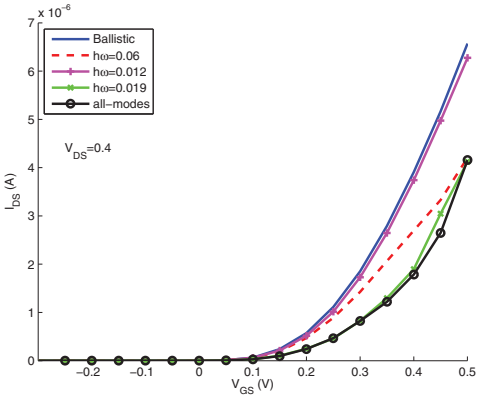

Fig. 3. I_{DS}-V_{GS} curve for different energies in optical phonon scattering mechanisms.

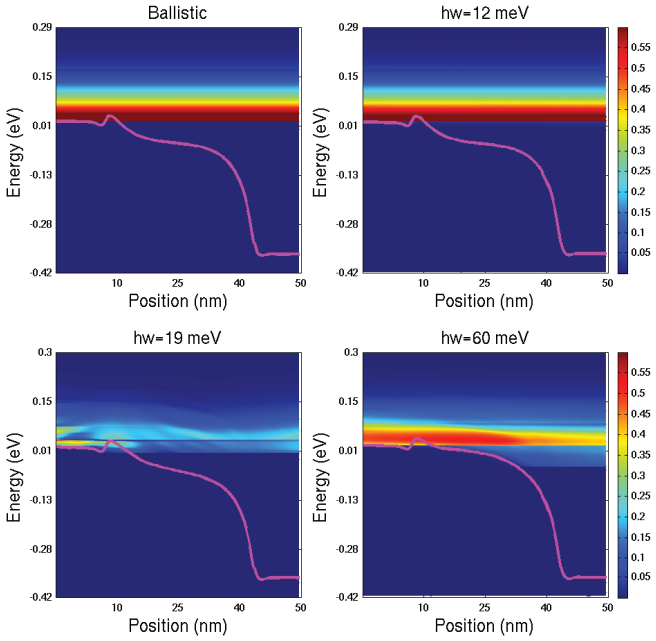

Fig. 4. Energy-resolved current density for ballistic transport and dissipative transport with different phonon energies. 19 meV phonons have reduced the current due to phonon absorption and back scattering of carriers. 60 meV phonons only spread the current spectrum by phonon emission without reducing the current magnitude.

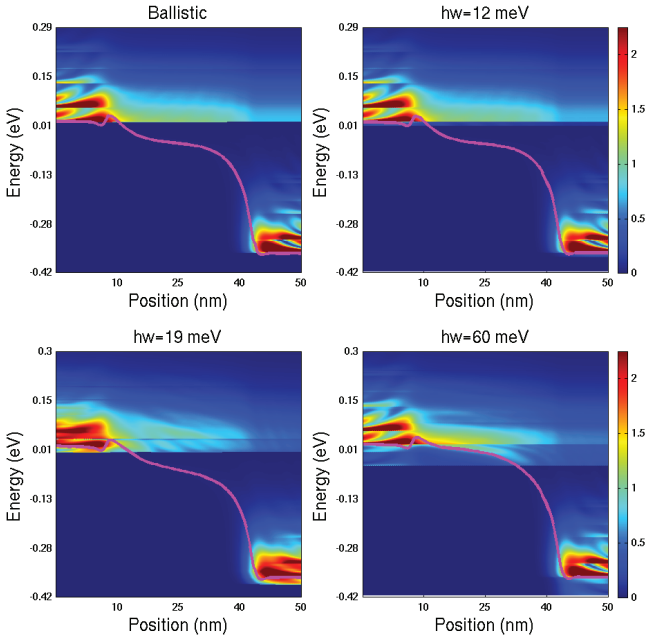

Fig. 5. Energy-resolved electron density density for ballistic transport and different g-type phonon energies. 19 mev phonons have reduced the charge density in the channel by phonon absorption. 60 meV phonons have increased and spread the charge spectrum to lower energies by phonon emission mechanism.

In order to establish a more detailed understanding between phonon energy and current reduction mechanisms, one should compare the current spectrum for different ranges of phonon energies and electron-phonon coupling elements in various cross section of the nanowire. This will give a deep understanding of parameters variation on quantum transport which will be the topic of future research work.

IV. Conclusion

We have investigated the effect of optical and acoustic phonon scattering on the electrical characteristics of multigate silicon nanowire in details. We found out that only *g*-type and acoustic phonons contribute to current reduction and for device dimensions considered here only *g*-type phonons are important. We also performed detailed study and comparison of on current and electron density spectrum for different *g*-type phonon energies. We found out that low-energy phonons are responsible for current reduction by phonon absorption while high-energy phonons increase the electron density by phonon emission without modifying the current magnitude considerably.

References

[1] L. Risch, "Pushing CMOS beyond the roadmap," *Solid-State Electronics*, vol. 50, pp. 527-535, Apr 2006.

[2] J. P. Colinge, "Quantum-wire effects in trigate SOI MOSFETs," *Solid-State Electronics*, vol. 51, pp. 1153-1160, 2007.

[3] J. Wang, E. Polizzi, and M. Lundstrom, "A three-dimensional quantum simulation of silicon nanowire transistors with the effective-mass approximation," *Journal of Applied Physics,* vol. 96, no. 4, pp. 2192-2203, 2004.

[4] R. Venugopal, M. Paulsson, S. Goasguen *et al.*, "A simple quantum mechanical treatment of scattering in nanoscale transistors," *Journal of Applied Physics,* vol. 93, no. 9, pp. 5613-5625, 2003.

[5] S. Jin, Y. J. Park, and H. S. Min, "A three-dimensional simulation of quantum transport in silicon nanowire transistor in the presence of electron-phonon interactions," *Journal of Applied Physics,* vol. 99, no. 12, 2006.

[6] M. Pourfath, H. Kosina, and S. Selberherr, "Numerical study of quantum transport in carbon nanotube transistors," *Mathematics and Computers in Simulation,* vol. 79, no. 4, pp. 1051-1059, Dec, 2008.

[7] S. O. Koswatta, S. Hasan, M. S. Lundstrom *et al.*, "Nonequilibrium green's function treatment of phonon scattering in carbon-nanotube transistors," *IEEE Transactions on Electron Devices,* vol. 54, no. 9, pp. 2339-2351, Sep, 2007.

[8] A. Afzalian, N. Dehdashti *et. al.*, "A new F(ast)-CMS NEGF algorithm for efficient 3D simulations of switching characteristics enhancement in constricted tunnel barrier silicon nanowire MuGFETs," *Journal of Computational Electronics*, vol. 8, no 3-4, pp. 1572-8137, 2009.

[9] M. Luisier and G. Klimeck, "Atomistic full-band simulations of silicon nanowire transistors: Effects of electron-phonon scattering," *Physical Review B*, vol. 80, Oct 2009.

[10] A. Svizhenko and M. P. Anantram, "Role of scattering in nanotransistors," *IEEE Transactions on Electron Devices*, vol. 50, pp. 1459-1466, Jun 2003.